European Journal of Medicinal Chemistry 62 (2013) 130–138

Contents lists available at SciVerse ScienceDirect

European Journal of Medicinal Chemistry

journal homepage: http://www.elsevier.com/locate/ejmech

Original article

Oxo-heterocyclic fused naphthalimides as antitumor agents: Synthesis and biological evaluation

Shaoying Tan [a,d], Hong Yin [b,d], Zhuo Chen [c,d,*], Xuhong Qian [a,b,d], Yufang Xu [a,b,c,d,*]

[a] State Key Laboratory of Bioreactor Engineering, East China University of Science and Technology, Shanghai 200237, China
[b] Shanghai Key Laboratory of Chemical Biology, East China University of Science and Technology, Shanghai 200237, China
[c] Shanghai Key Laboratory of New Drug Design, East China University of Science and Technology, Shanghai 200237, China
[d] School of Pharmacy, East China University of Science and Technology, Shanghai 200237, China

ARTICLE INFO

Article history:
Received 27 August 2012
Received in revised form
23 November 2012
Accepted 23 December 2012
Available online 3 January 2013

Keywords:
Oxo-heterocyclic
Naphthalimides
Antitumor agents
Topo I
Topo II
DNA intercalation

ABSTRACT

Three series of novel oxo-heterocyclic fused naphthalimide derivatives (**8a**–**8f**, **13a**–**13d**, **17a**–**17d**) were prepared. The newly-synthesized compounds, and their thio-heterocyclic fused analogs (**1a**–**1c**, **2a**–**2d**, **3a**–**3c**) exhibited potent antiproliferative activity correlated well with their structure. Further research demonstrated that all the representative compounds **13a**, **2a** and **17a**, **3a** showed strong inhibition activity to topo II similarly with amonafide, and also potent topo I inhibition activity, which was seldom reported before for naphthalimide derivatives. Preliminary exploration proved their DNA sequence preference. In all, dual topo I/topo II inhibition and DNA sequence preference might contribute to enhancing tumor selectivity and overcoming drug resistance.

1. Introduction

In the past decade, DNA targeted antitumor agents remain the cornerstone for cancer therapy despite the emerging of drugs with different mechanisms of action. Great efforts have been made to explore novel agents with better specificity and efficacy, as non-specific cytotoxicity was the Achilles' heel of conventional DNA-interactive drugs [1,2]. The specificity could be acquired by targeting protein-DNA complex. For example, the clinical effective drugs, like Doxorubicin and Etoposide, could stabilize topoisomerase II-DNA cleavable complex. Irinotecan (Camptosar, CPT-11) and Topotecan (Hycamtin), derivatives of the plant alkaloid, act on topoisomerase I [3]. Another strategy was to explore sequence selective DNA binding agents. For example, derivatives of Netropsin, could bind to the AT-rich sequences in double stranded DNA and showed potent selectivity to tumor cells.

Naphthalimide derivatives, first designed by Braña et al. in 1973 [4], are a typical type of intercalators, which normally contain a flat aromatic or heteroaromatic moiety and basic side chains. Amonafide [5] is one of the most widely studied naphthalimides, which binds DNA by intercalation and poisons Topoisomerase II as reported, and shows excellent activity in clinical phase II breast cancer trials [6–9]. But it failed in clinical phase III trials because of its unpredictable side effects on dose-limiting bone marrow toxicity due to its metabolization to *N*-acetyl-amonafide. Accordingly, many derivatives were synthesized. Remers group put forward an effective modified method by fusing rings on the naphthalene moiety and obtained novel naphthalimides with the IC_{50} values up to 7 nM against L1210 [10,11]. Braña group have reported sulfonated, pyrazine, furan, thiophene-fused naphthalimides, which could induce 10 folds more potent cytotoxicity comparing with amonafide [12–14]. Besides, N-substitution naphthalimides with thiourea, amide and urea were synthesized by Kiss group and increased the maximum tolerated dose to 3–4 folds [5].

Our group also made significant attempts in synthesizing heterocyclic-fused naphthalimides to enhance cytotoxicity. For

Abbreviations: CD, circular dichroism; CPT, camptothecin; ctDNA, calf thymus DNA; kDNA, kinetoplast DNA; SAR, structure–activity relationship.

* Corresponding authors. School of Pharmacy, East China University of Science and Technology, Shanghai 200237, China. Tel.: +86 21 64251399; fax: +86 21 64252603.
E-mail addresses: chenzhuo@ecust.edu.cn (Z. Chen), yfxu@ecust.edu.cn (Y. Xu).

0223-5234/$ – see front matter © 2013 Elsevier Masson SAS. All rights reserved.
http://dx.doi.org/10.1016/j.ejmech.2012.12.039

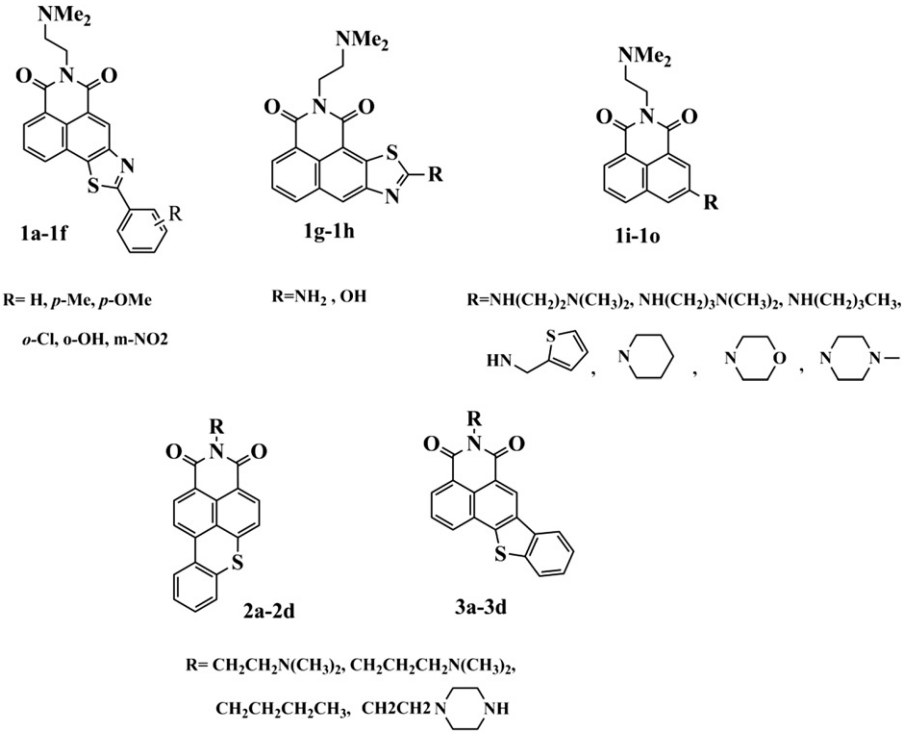

Fig. 1. Naphthalimides derivatives reported in our group.

example, linear and angular thiazonaphthalimides (Fig. 1 **1a**–**1h**) were reported by Li et al. with IC_{50} values up to 0.8 nM against A549 [15–17]. Xie et al. synthesized N-substitution amonafide derivatives (Fig. 1 **1i**–**1o**), which showed improved antitumor activity over amonafide and were supposed to avoid the side effects of amonafide [18]. Besides, the thio-heterocyclic fused naphthalimides (Fig. 1 **2a**–**2d**, **3a**–**3d**) were reported as high efficient DNA photocleaver [19,20], and have not yet been characterized as cytotoxic agents except for **3a**.

Recently, amonafide reentered phase III clinical trial against secondary acute myeloid leukemia, which encouraged us to develop naphthalimide derivatives as potential antitumor drugs. Previously reported naphthalimide derivatives of our group were normally thio-heterocyclic fused naphthalimides. In this paper, oxo-heterocyclic fused naphthalimides (Fig. 2) were synthesized for establishing better structure–activity relationship (SAR). These novel-synthesized compounds, as well as part of their thio-heterocyclic fused analogs (**1a**–**1c**, **2a**–**2d**, **3a**–**3d**) were evaluated of their antiproliferative activity from DNA intercalation, inhibition of topo I and II in comparison with amonafide.

2. Chemistry

As shown in Scheme 1, the critical intermediates **7a**–**7f** were prepared as we have reported previously [21]. They were synthesized from 4-bromo-3-nitro-naphthalimide **4** via substitution, reduction as well as cyclization in the existence of PPA. The target compounds **8a**–**8f** were then obtained by **7a**–**7f** condensed with *N*′,*N*′-dimethylethane-1,2-diamine.

As for **13a**–**13d**, the critical intermediate **12** were synthesized from 4-bromo-naphthalimide as reported (see Scheme 2) [22,23]. Compound **12** was obtained by 4-bromo-naphthalimide **10** substituted with o-amino phenol, reduced with Fe/acetic acid, and then cyclized by Diazo reaction and Pschorr reaction. The target compounds **13a**–**13d** were obtained from corresponding aminos condensed with **12**.

A similar synthesis strategy was implicated for **17a**–**17d** as shown in Scheme 3 [23], only that the synthesis started from 4-bromo-3-nitro-naphthalimide. The critical intermediate **16** was mixed with corresponding aminos to give the target compounds **C1**–**C4**.

3. Results and discussion

3.1. Antitumor activity in vitro

The antitumor activities of oxo- and thio-heterocyclic fused naphthalimides were evaluated *in vitro* against tumor cell lines A549 (human lung cancer cell), P388 (murine leukemia cell) and

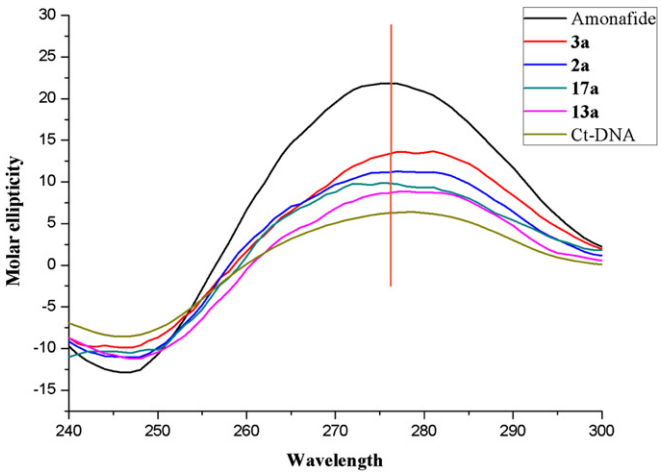

Fig. 2. CD spectra of ctDNA (100 μM) incubated with target compounds (20 μM).

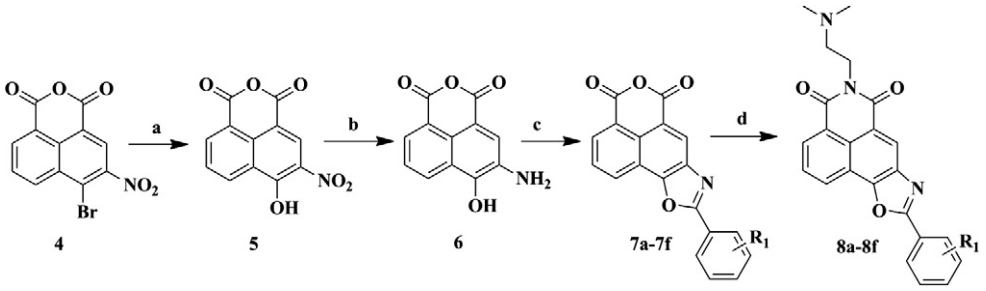

Scheme 1. Syntheses of target compounds **8a**–**8f**. (a) NaOH, 80 °C, 8 h; (b) $SnCl_2$, HCl, 80 °C 2 h (c) substituted carboxylic acids, PPA, 120 °C, 5 h; (d) *N*′,*N*′-dimethylethane-1,2-diamine, ethanol, reflux, 3 h.

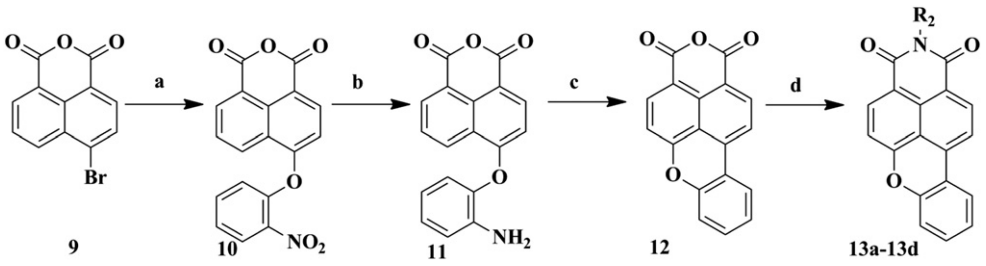

Scheme 2. Syntheses of target compounds **13a**–**13d**. (a) *o*-nitrophenol, NaOH, DMF, Cu, reflux 1 h; (b) Fe, acetic acid, reflux, 1 h. (c) HCl, acetic acid, $NaNO_2$ 0–5 °C, $CuSO_4$, HAc, H_2O. (d) R_2NH_2, ethanol, reflux 3 h.

normal cell lines LO2 (human liver cell), respectively, as listed in Tables 1 and 2.

Among **8a**–**8f**, it was found from Table 1 that compounds **8a**, **8c** and **8f** exhibited potent antiproliferative activities, which was comparable with amonafide. Compounds with electron-donating groups provided more antitumor efficacy, such as **8c** vs **8e**. Besides, substitution on the ortho-position induced better cytotoxicity than the substitution on the para-position, for example, **8f** was 7.6 folds more potent than **8c** against A549. Similar SAR were observed for their sulfur-containing analogs, except that they are more potent antitumor agents, e.g. **1c** vs **8c**.

As for **13a**–**13d** and **17a**–**17d**, the antiproliferative potency varied from the substitution of the condensed aminos. *N*′,*N*′-dimethylethane-1,2-diamine derivatives **13a**, **17a** were generally more potent than their analogs, which was in consistence with previous reported naphthalimide-derived DNA intercalators. Extension of linker or increasing rigidity of amino group would normally reduce the cytotoxicity. For example, **13b** and **13d** exhibited much decreased antiproliferative activity against A549 with IC_{50} values at 98.26 μM and 28.95 μM, respectively. Besides, it was quite interesting to observe compounds **13c** and **17c** without amino side chain exhibited potent antiproliferative activities against A549. Since they were not typical DNA intercalators in structure, other mechanism of action was probably involved, which would not be discussed in this article. Similar SAR were observed for their sulfur-containing analogs (**2a**–**2d** and **3a**–**3d**), which normally induced enhanced cytotoxicity. Compounds **2a** and **3a** exhibited significant antiproliferative activity with IC_{50} values at 0.14 and 0.007 μM for A549 respectively. Besides, compounds **2b** and **3b** also possessed efficient antitumor activities. Moreover, **2c** and **3c** induced potent antiproliferative activates against both A549 and P388.

Considering the shortcoming of cytotoxic compounds, the newly-synthesed compounds (**8a**–**8f**, **13a**–**13d**, **17a**–**17d**) and compounds (**2a**, **3a**) were selected to evaluate their cytotoxicity against the normal cell line LO2 (Table 1). Less cytotoxicity against the normal cell line in contrast to tumor cell lines, or certain tumor specificity was observed.

3.2. DNA intercalating studies by circular dichroism (CD) spectra

As **13a**, **2a**, **17a**, **3a** exhibited potent cytotoxicity and moderate specificity in antiproliferative assay, their mechanism of action was investigated. Firstly, the CD spectroscopy was applied for the interaction with DNA, as typical intercalating agents could induce calf thymus DNA's (ctDNA) conformation changes [24]. As shown in Fig. 2, amonafide could induce significant changes in a negative peak around 245 nm caused by the helical B conformation and in a positive peak around 275 nm due to base stacking, which was consistent with literature. All the representative compounds could

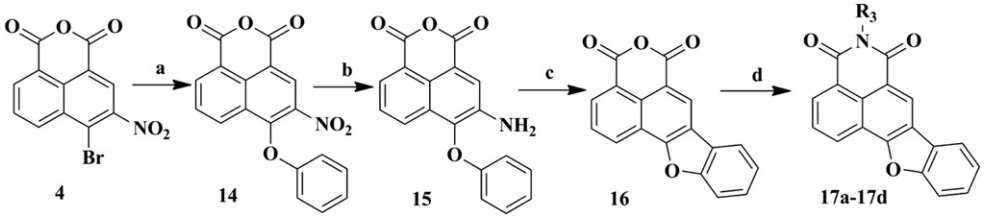

Scheme 3. Syntheses of target compounds **17a**–**17d**. (a) pyridine, phenol, NaH, Cu, reflux 5 h; (b) $SnCl_2$, HCl, 80 °C 2 h; (c) HCl, acetic acid, $NaNO_2$ 0–5 °C, $CuSO_4$, HAc, H_2O (d) R_2NH_2, ethanol, reflux 3 h.

Table 1
SAR of oxo-heterocyclic fused naphthalimides and their sulfur-containing analogues.

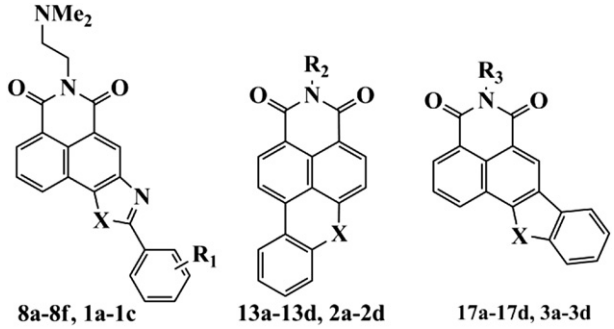

8a-8f, 1a-1c 13a-13d, 2a-2d 17a-17d, 3a-3d

Compounds	R=	X	Cytotoxicity (IC_{50}, μM)		
			A549[a]	P388[b]	LO2[a]
8a	R_1 = H	O	0.53	2.50	3.0
8b	R_1 = *p*-Me	O	34.70	19.30	6.7
8c	R_1 = *p*-OMe	O	6.60	1.29	3.4
8d	R_1 = *p*-Cl	O	72.40	20.10	>100
8e	R_1 = *p*-NO_2	O	17.80	100.00	>100
8f	R_1 = *o*-OMe	O	0.89	1.30	1.9
1a	R_1 = H	S	0.085	0.66	N.d.[c]
1b	R_1 = *p*-Me	S	0.42	0.62	N.d.
1c	R_1 = *p*-OMe	S	0.016	0.43	N.d.
13a	$R_2 = CH_2CH_2N(CH_3)_2$	O	0.61	1.11	4.1
13b	$R_2 = CH_2CH_2CH_2N(CH_3)_2$	O	98.26	3.50	10.3
13c	$R_2 = CH_2CH_2CH_2CH_3$	O	5.39	>100	>100
13d	R_2= 	O	28.95	4.52	11.5
2a	$R_2 = CH_2CH_2N(CH_3)_2$	S	0.14	1.58	4.1
2b	$R_2 = CH_2CH_2CH_2N(CH_3)_2$	S	0.19	0.63	N.d.
2c	$R_2 = CH_2CH_2CH_2CH_3$	S	0.87	1.20	N.d.
2d	R_2= 	S	100.00	>100	N.d.
17a	$R_3 = CH_2CH_2N(CH_3)_2$	O	0.36	0.65	5.0
17b	$R_3 = CH_2CH_2CH_2N(CH_3)_2$	O	0.74	0.17	6.6
17c	$R_3 = CH_2CH_2CH_2CH_3$	O	1.40	>100	>100
17d	R_3= 	O	>100	0.58	11.9
3a	$R_3 = CH_2CH_2N(CH_3)_2$	S	0.007	0.26	0.9
3b	$R_3 = CH_2CH_2CH_2N(CH_3)_2$	S	0.25	0.32	N.d.
3c	$R_3 = CH_2CH_2CH_2CH_3$	S	1.35	0.74	N.d.
3d	R_3= 	S	11.75	72.44	N.d.
Amonafide			1.10	0.20	5.0

[a] Cytotoxicity (CTX) against human lung cancer cell (A549) and human liver cell (LO2) was measured by sulforhodamine B dye-staining method.
[b] CTX against murine leukemia cells (P388) was measured by microculture tetrazolium-formazan method.
[c] Not determined.

induce the conformational changes, which supported their intercalating capacity, but were much weaker than amonafide. In detail, the thio-heterocyclic fused naphthalimides (**2a**, **3a**) showed stronger changes in the corresponding position than the oxo-heterocyclic fused naphthalimides (**13a**, **17a**). Thus, the sulfur-containing derivatives were more potent DNA intercalators than the oxygen-containing analogs, which was in consistence with their cytotoxic superiority.

Table 2
Association constants (*Ka*'s, M^{-1}) of **13a**, **2a** and **17a**, **3a** with polydeoxynucleotides.[a,b]

DNA/compds	**13a**	**2a**	**17a**	**3a**
Poly (dAdT)·Poly (dAdT)	1.32×10^5	4.48×10^5	5×10^6	8×10^6
Poly (dGdC)·Poly (dGdC)	6.89×10^5	4.76×10^6	6.36×10^6	7.6×10^7

[a] A measurement by fluorospectrometric methods in 20 mM sodium phosphate buffer (pH 7.0) at room temperature (20 ± 1 °C). The concentrations of compounds and polydeoxynucleotides were 3×10^{-6} and $0–6.32 \times 10^{-5}$ M, respectively.
[b] These values were derived from the experimental data by nonlinear curve fitting methods using Microcal Origin software (version 8.0).

3.3. Fluorescent spectra studies

For further research for the interaction of the representative compounds with DNA, the association steady constants (Kb) were measured according to the quenching of fluorescence following the increasing concentrations of ctDNA. Fig. 3 showed the fluorescence of the compound before and after the addition of ctDNA (**2a** as an example), which exhibited that the fluorescence intensity of **2a** quenched rapidly with the addition of ctDNA [25,26]. From the analyses on the relationship between the fluorescence intensities and the DNA concentrations by nonlinear curve fitting methods, the association steady constants of the compounds (**13a**, **2a**, **17a**, **3a**) were available at 1.45×10^5, 9.70×10^4, 2.89×10^5 and 1.10×10^5 M^{-1}, respectively (Figure S1). It indicated that the thio-heterocyclic analogs exhibited enhanced ability of DNA-interaction (e.g. **13a** vs **2a**), which is consistent with cytotoxicity and CD spectroscopy.

3.4. Topo II inhibition assay

Topo II, the important target enzyme of antitumor chemotherapy, is related with mitotic chromosome pairing, chromosome segregation, gene recombination and transcription, DNA manipulation and restoration etc [27]. Amonafide was an important DNA intercalator and could inhibit topo II by forming and stabilizing a ternary drug-DNA-topoisomerase complex [28]. The kinetoplast DNA (kDNA) assay was introduced based on specific decatenation of kDNA by topo II. As shown in Fig. 4, all the representative compounds decrease the amount of released decatenated kDNA minicircles, and thus were capable of inhibiting topo II activity. Compounds **13a**, **17a** and **3a** exhibited similar topo II inhibition efficacy as amonafide at the tested concentration. Besides, all the naphthalimides exhibited stronger activity than Etoposide (VP-16), a famous topo II inhibitor.

3.5. Topo I inhibition assay

Topo I, another member of topoisomerase family, was associated with the process of DNA replication, transcription and recombinant etc and caused a short DNA single-strand breaks via the formation of intermediates in the catalytic process [3]. The research of topo I inhibitory activity was implicated in conventional chemotherapy agents. As shown in Fig. 5, the topo I inhibitor camptothecin (CPT) could reduce topo I-induced pBR322 relaxation [29]. It is quite exciting that all the naphthalimides including amonafide, exhibited stronger inhibitory activity to topo I than camptothecin (CPT). Besides, compound **2a** was relatively weaker than its analogs.

Existing topoisomerase-targeting clinical drugs, such as camptothecin and podophyllotoxin derivatives, formed topo-DNA complexes with either topo I or topo II. These drugs have a fatal flaw in drug resistance which limited their clinical use. As reported, the

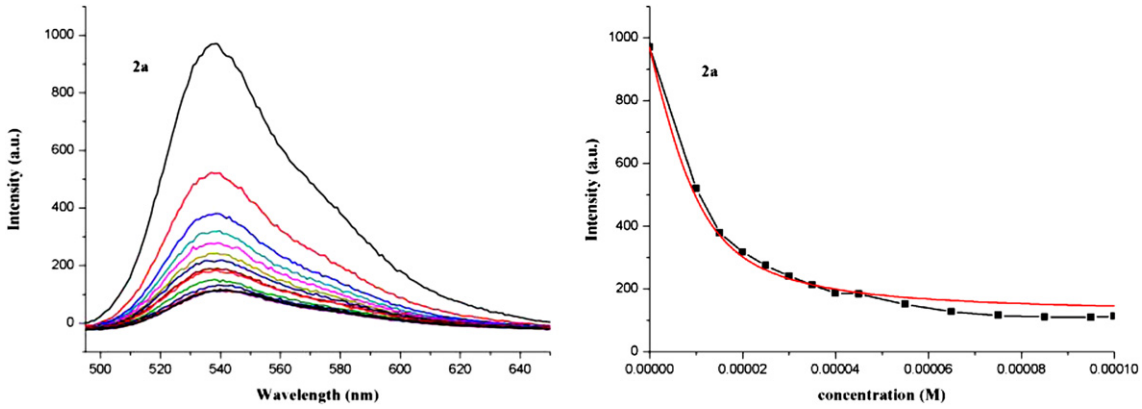

Fig. 3. Fluorescence spectra of **2a** (10 μM) with ctDNA. The concentrations of ctDNA were increased from 0 to 100 μM in 20 mM tris–HCl (pH 7.5) at 25 °C. The insets indicated the relationship between the fluorescent intensity and the concentration of ctDNA (μM).

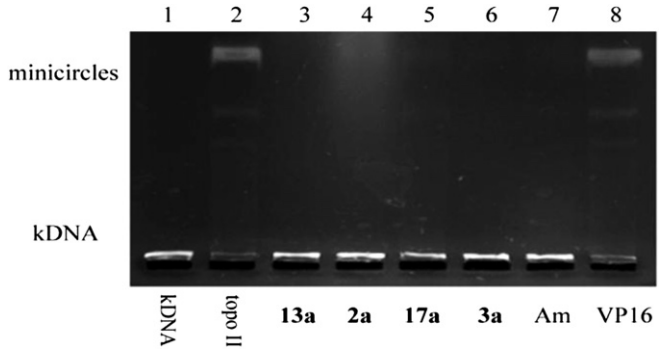

Fig. 4. Inhibition of topo II-mediated kDNA decatenation by target compounds (100 μM). Lane 1, kDNA; lane 2, minicircles (no drug); lanes 3–8, compounds **13a**, **2a**, **17a**, **3a**, amonafide, and Etoposide (VP-16), respectively.

resistance could be abated in case of inhibiting both topo I and topo II activity [30]. Thus, it is probably that naphthalimides have advantages in overcoming drug resistance.

3.6. DNA sequence preference

According to previous report, amonafide exhibited GC sequence preference, which would contribute to its tumor selectivity [31]. Accordingly, we investigated the sequence preference of oxo-heterocyclic fused compounds and their thio analogs. The binding affinities of compounds **13a**, **2a**, **17a** and **3a** with poly[dA-dT]·poly[dA-dT], poly[dG-dC]·poly[dG-dC] were listed in Table 2. The association constants of **2a** and **3a** with poly[dG-dC]·poly[dG-dC] were 10 folds higher than poly[dA-dT]·poly[dA-dT]. The GC sequence preference was also observed for **13a** and **17a** though not so potent as their sulfur-containing analogs.

Preliminary exploration was carried out to provide further insight into the precise sequence selectivity [32,33]. The association constants of **13a** and **2a** with seven designed double-strand oligodeoxynucleotides were measured (Table S1). Compound **2a** exhibited 4–111 folds selectivity against the sequence 5′-TGCGCA-3′/3′-ACGCGT-5′. Researches on selectivity for core sequences associated with tumor progression are still going on.

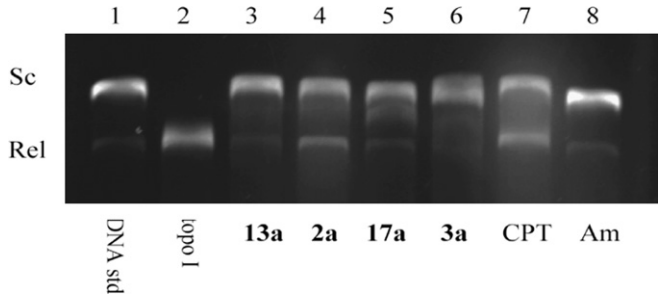

Fig. 5. Inhibition of topo I-mediated DNA std (pBR322) decatenation by target compounds (100 μM except for CPT 200 μM). Lane 1, DNA std; lane 2, topo I (no drug); lanes 3–8, compounds **13a**, **2a**, **17a**, **3a**, camptothecin (CPT) and amonafide, respectively.

4. Conclusions

In this article, three series of novel oxo-heterocyclic fused naphthalimides were synthesized and evaluated of their antitumor potency in comparison with their thio-heterocyclic analogs. The newly-synthesized compounds exhibited more potent antiproliferative activity than amonafide, though they were relatively less potent than their sulfur-containing analogs. Representative compounds **13a**, **2a**, **17a** and **3a** were then investigated of their antitumor mechanism of action. These compounds acted as DNA intercalators, but were much weaker than amonafide according to the results of CD. The sulfur-containing analogs exhibited better DNA affinity which was consistent with their antiproliferative potency. Furthermore, the tested compounds could induce significant inhibition activity to both topo II and topo I in cell-free system. The tested compounds also exhibited GC sequence preference, and certain sequence selectivity against designed double-strand oligodeoxynucleotides. In all, dual topo I/topo II inhibition and DNA sequence preference might contribute to enhancing tumor selectivity and overcoming drug resistance.

5. Experimental section

All the solvents were of analytic grade. ctDNA and polydeoxynucleotides (poly[dG-dC]·poly[dG-dC] and poly[dA-dT]·poly[dA-dT]) were products of Amersham Biosciences and Sigma Chemicals Co., respectively. Calf thymus DNA, polydeoxynucleotides and oligodeoxynucleotides were used without further purification. ^{1}H NMR and ^{13}C NMR were measured on a Bruker AV-400 spectrometer with chemical shifts reported as parts per million (in CD_3OD/DMSO-d_6/$CDCl_3$, TMS as an internal standard). Mass spectra were measured on a HP 1100 LC-MS spectrometer. Melting points were determined by an X-6 micro-melting point apparatus and uncorrected. Absorption spectra

were determined on PGENERAL TU-1901 UV–vis Spectrophotometer. Milli-Q water (Millipore Co.) was used throughout the whole experiments.

5.1. Synthesis

5.1.1. 4-Bromo-3-nitro-1,8-naphthalic anhydride (**4**) [34]

Sodium nitrate (2.6 g, 0.03 mol) was added to 4-bromo-1,8-naphthalic anhydride (7.0 g, 0.025 mol) in concentrated sulfuric acid (37.5 mL) within 1 h. Stirred for 2 h in room temperature, the solution was poured into water (500 mL) and the precipitate was filtered, washed with water and recrystallized from acetic acid to obtain compound **4**. Yellow solid, yield: 79%; m.p. 233–235 °C (m.p. 233–234 °C in literature). ^{1}H NMR (400 MHz, *DMSO*-d_6) (ppm): 8.90 (s, 1H), 8.80 (d, J = 8.4 Hz, 1H), 8.73 (d, J = 7.2 Hz, 1H), 8.17 (t, J = 7.2 Hz, 1H). ^{13}C NMR (100 MHz, *DMSO*-d_6) (ppm): 160.1, 159.5, 149.8, 135.7, 135.4, 131.4, 130.9, 126.0, 122.3, 121.4, 120.8.

5.1.2. 4-Hydroxyl-3-nitro-1,8-naphthalic anhydride (**5**) [34]

4 (32.2 g, 0.1 mol) was stirred in 20% aqueous sodium hydroxide (200 mL) for 8 h at 80–85 °C. The dark red solution was cooled and poured into ice-cold 10% hydrochloric acid (500 mL), stirred and filtered to obtain pale yellow residue. The crude product was washed and recrystallized from glacial acetic acid to give compound **5**. Pale yellow needle, yield: 85%; m.p. 289–290 °C (m.p. 288–289 °C in literature). ^{1}H NMR (400 MHz, *DMSO*-d_6) (ppm): 8.74 (s, 1H), 8.65 (d, J = 8.0 Hz, 1H), 8.43 (d, J = 7.2 Hz, 1H), 7.71 (t, J = 7.6 Hz, 1H). ^{13}C NMR (100 MHz, *DMSO*-d_6) (ppm): 162.4, 161.4, 160.0, 134.7, 133.7, 132.8, 132.5, 131.2, 128.2, 126.9, 119.0, 103.5.

5.1.3. 4-Hydroxyl-3-amino-1,8-naphthalic anhydride (**6**) [34]

A mixture of **5** (15 g, 0.058 mol), tin (II) chloride (50 g, 0.26 mol) and concentrated hydrochloric acid (80 mL) was stirred for 2 h at 80 °C. The suspension was cooled and filtered. The residue was washed with 5% hydrochloric acid and water, dried and recrystallized from pyridine. Orange–yellow needles, yield: 66%; m.p. >340 °C (m.p. >340 °C in literature). ^{1}H NMR (400 MHz, *DMSO*-d_6) (ppm): 8.50 (d, J = 8.4 Hz, 1H), 8.21 (d, J = 6.8 Hz, 1H), 8.07 (s, 1H), 7.63 (t, J = 8.0 Hz, 1H). ^{13}C NMR (100 MHz, *DMSO*-d_6) (ppm): 162.4, 160.9, 129.8, 129.6, 125.5, 124.9, 124.4, 118.6.

5.1.4. General procedure for the preparation of **7a**–**7f** [34]

The PPA (35 mL), **6** (0.8 g, 0.0035 mol) and corresponding benzoic acid (0.011 mol) was mixed and stirred at 135 °C. After 4 h, the solution was cooled and poured into the ice water (350 mL), the precipitate was filtered, washed with water and dried for direct use in the next step. Yellow solid, yield: 60.9–68.7%.

5.1.5. General procedure for the preparation of **8a**–**8f**

The corresponding intermediates **7a**–**7f** (0.001 mol) were dissolved in 20 mL ethanol. After adding *N*,*N*-dimethylethylenediamine (0.163 mL, 0.0015 mol), the mixture were stirred and refluxed for 2–3 h, then the solution was evaporated in vacuum and the residue was purified on silica gel chromatography.

5.1.5.1. N-(N′,N′-dimethylamine-ethyl)-9-phenyl-oxazole[4,5-c] naphthalimide (**8a**).

Pale yellow solid, yield: 92%, m.p. 172–173 °C. ^{1}H NMR (400 MHz, *CDCl*$_3$) (ppm): 9.01 (s, 1H), 8.69–8.64 (m, 2H), 8.36 (d, J = 5.6 Hz, 2H), 7.92 (t, J = 8.0 Hz, 1H), 7.62 (d, J = 5.6 Hz, 2H), 7.29 (s, 1H), 4.40 (t, J = 7.2 Hz, 2H), 2.76 (t, J = 6.8 Hz, 2H), 2.43 (s, 6H). ^{13}C NMR (100 MHz, *CDCl*$_3$) (ppm): 164.2, 164.1, 163.8, 150.1, 139.5, 132.2, 130.6, 129.2, 127.8, 127.7, 126.7, 126.4, 126.3, 125.1, 123.4, 120.3, 118.4, 56.9, 45.7, 38.2. IR (KBr): 2755, 2344, 1700, 1650, 1338, 773 cm^{-1}. HR-MS: $C_{23}H_{19}N_3O_3$ calculated: 385.1426, found: 385.1441.

5.1.5.2. N-(N′,N′-dimethylamine-ethyl)-9-(4′-methyl-phenyl)-oxazole[4,5-c] naphthalimide (**8b**).

Pale yellow solid, yield: 84%, m.p. 230–231 °C. ^{1}H NMR (400 MHz, *CDCl*$_3$) (ppm): 9.00 (s, 1H), 8.66 (t, J = 8.8 Hz, 2H), 8.25 (d, J = 7.6 Hz, 2H), 7.92 (t, J = 8.0 Hz, 1H), 7.41 (d, J = 7.6 Hz, 2H), 4.42 (t, J = 5.6 Hz, 2H), 2.82 (t, J = 5.6 Hz, 1H), 2.51 (s, 3H), 2.48 (s, 6H). ^{13}C NMR (100 MHz, *CDCl*$_3$) (ppm): 164.5, 164.2, 163.9, 150.0, 142.9, 139.6, 130.5, 129.9, 127.8, 127.6, 126.6, 126.4, 125.1, 123.6, 123.4, 120.1, 118.4, 56.7, 45.4, 37.9, 21.7. IR (KBr): 3287, 2820, 2774, 2369, 1660, 1330, 773 cm^{-1}. HR-MS: $C_{24}H_{21}N_3O_3$ calculated: 399.1583, found: 399.1564.

5.1.5.3. N-(N′,N′-dimethylamine-ethyl)-9-(4′-methoxy-phenyl)-oxazole[4,5-c] naphthalimide (**8c**).

Pale yellow solid, yield: 86%, m.p. 213–214 °C. ^{1}H NMR (400 MHz, *CDCl*$_3$) (ppm): 8.96 (s, 1H), 8.65 (d, J = 7.6 Hz, 1H), 8.61 (d, J = 8.0 Hz, 1H), 8.27 (d, J = 8.0 Hz, 2H), 7.90 (t, J = 7.6 Hz, 1H), 7.08 (d, J = 8.4 Hz, 2H), 4.39 (t, J = 6.8 Hz, 2H), 3.95 (s, 3H), 2.74 (t, J = 6.8 Hz, 2H), 2.42 (s, 6H). ^{13}C NMR (100 MHz, *CDCl*$_3$) (ppm): 164.4, 164.2, 163.9, 162.8, 149.9, 139.7, 130.3, 129.6, 127.5, 126.4, 126.3, 124.9, 123.4, 120.0, 118.7, 118.3, 114.6, 56.9, 55.6, 45.7, 38.3. IR (KBr): 2950, 2771, 2349, 1690, 1655 cm^{-1}. HR-MS: $C_{24}H_{21}N_3O_4$ calculated: 415.1532, found: 415.1538.

5.1.5.4. N-(N′,N′-dimethylamine-ethyl)-9-(4′-chloro-phenyl)-oxazole [4,5-c] naphthalimide (**8d**).

Pale yellow solid, yield: 85%, m.p. 191–192 °C. ^{1}H NMR (400 MHz, *CDCl*$_3$) (ppm): 9.03 (s, 1H), 8.70 (d, J = 7.2 Hz, 1H), 8.66 (d, J = 8.0 Hz, 1H), 8.32 (d, J = 8.4 Hz, 2H), 7.94 (t, J = 8.0 Hz, 1H), 7.60 (d, J = 8.4 Hz, 2H), 4.42 (t, J = 5.6 Hz, 2H), 2.78 (t, J = 5.6 Hz, 2H), 2.45 (s, 6H). ^{13}C NMR (100 MHz, *CDCl*$_3$) (ppm): 164.1, 163.8, 163.3, 150.1, 139.5, 138.6, 130.7, 129.6, 129.0, 127.8, 126.8, 126.4, 125.1, 124.8, 123.5, 120.5, 118.4, 56.9, 45.6, 38.2. IR (KBr): 3081, 2931, 2758, 1703, 1657, 1341, 780 cm^{-1}. HR-MS: $C_{23}H_{18}N_3O_3Cl$ calculated: 421.1007, found: 421.0974.

5.1.5.5. N-(N′,N′-dimethylamine-ethyl)-9-(4′-nitro-phenyl)-oxazole [4,5-c] naphthalimide (**8e**).

Pale yellow solid, yield: 94%, m.p. 205–206 °C. ^{1}H NMR (400 MHz, *CDCl*$_3$) (ppm): 9.06 (s, 1H), 8.73 (d, J = 7.2 Hz, 1H), 8.70 (d, J = 8.0 Hz, 1H), 8.58 (d, J = 8.4 Hz, 2H), 8.48 (d, J = 8.0 Hz, 2H), 7.98 (t, J = 8.0 Hz, 1H), 4.40 (t, J = 5.6 Hz, 2H), 2.75 (t, J = 5.6 Hz, 2H), 2.42 (s, 6H). ^{13}C NMR (100 MHz, *CDCl*$_3$) (ppm): 164.0, 163.6, 161.8, 150.4, 149.8, 139.4, 131.9, 131.1, 128.1, 127.2, 126.4, 125.3, 124.5, 123.6, 121.0, 118.4, 57.0, 45.7, 38.4. IR (KBr): 3065, 2945, 2777, 1696, 1334, 780 cm^{-1}. HR-MS: $C_{23}H_{18}N_4O_5$ calculated: 428.1277, found: 428.1277.

5.1.5.6. N-(N′,N′-dimethylamine-ethyl)-9-(2′-methoxy-phenyl)-oxazole[4,5-c] naphthalimide (**8f**).

Pale yellow solid, yield: 90%, m.p. 213–214 °C. ^{1}H NMR (400 MHz, *CDCl*$_3$) (ppm): 9.09 (s, 1H), 8.68 (t, J = 7.6 Hz, 2H), 8.28 (d, J = 8.0 Hz, 1H), 7.92 (t, J = 8.0 Hz, 1H), 7.61 (t, J = 7.6 Hz, 1H), 7.24–7.13 (m, 2H), 4.44 (t, J = 5.6 Hz, 2H), 4.11 (s, 3H), 2.85 (t, J = 5.6 Hz, 2H), 2.50 (s, 6H). ^{13}C NMR (100 MHz, *CDCl*$_3$) (ppm): 164.3, 164.0, 162.8, 158.7, 149.8, 139.6, 133.5, 131.3, 130.5, 127.5, 126.7, 125.5, 123.3, 120.9, 119.9, 118.3, 115.3, 112.3, 56.7, 56.3, 45.4, 37.8. IR (KBr): 2953, 2774, 2357, 1699, 1657, 773 cm^{-1}. HR-MS: $C_{24}H_{21}N_3O_4$ calculated: 415.1532, found: 415.1548.

5.1.6. 4-(2-Nitrophenoxy)-1,8-naphthalic anhydride (**10**) [35]

A mixture of 4-bromonaphthalic anhydride **9** (1.02 g, 0.0037 mol), *o*-nitrophenol (0.34 g, 0.0024 mol), sodium hydroxide (0.025 g) and copper powder (0.04 g) was mixed and refluxed in DMF (45 mL) for 1 h. The solution was cooled and hydrochloric acid (7.5 mL 20%) was added. Then the precipitate was filtered and recrystallized from acetic acid. Pale yellow solid, yield: 82%, m.p. 268–269 °C (m.p. 266–268 °C in literature). ^{1}H NMR (400 MHz, *DMSO*-d_6) (ppm): 8.79 (d, J = 8.4 Hz, 1H), 8.63 (d, J = 7.2 Hz, 1H), 8.45 (d, J = 8.4 Hz, 1H), 8.29 (d, J = 8.4 Hz, 1H), 8.00 (t, J = 8.0 Hz,

1H), 7.95 (t, J = 7.6 Hz, 1H), 7.67 (d, J = 4.8 Hz, 2H), 7.07 (d, J = 8.0 Hz, 1H). ^{13}C NMR (100 MHz, *DMSO-d_6*) (ppm): 161.3, 160.5, 159.3, 146.9, 142.2, 136.6, 134.9, 133.8, 131.9, 129.7, 128.3, 127.8, 127.0, 124.9, 123.4, 119.8, 114.2, 111.1.

*5.1.7. 4-(2-Aminophenoxy)-1,8-naphthalic anhydride (**11**) [35]*

A mixture of compound **10** (0.25 g, 0.0008 mol) and iron powder (0.12 g, 0.002 mol) was refluxed in glacial acetic acid (10 mL) for 1 h. The brown solution was cooled and water (30 mL) was added. The precipitate was filtered and washed with water. Yellow solid, yield: 94%, m.p. 172–174 °C (m.p. 171–172 °C in literature). ^{1}H NMR (400 MHz, *DMSO-d_6*) (ppm): 8.89 (d, J = 8.4 Hz, 1H), 8.60 (d, J = 5.2 Hz, 1H), 8.46 (d, J = 8.0 Hz, 1H), 7.96 (t, J = 7.2 Hz, 1H), 7.10 (t, J = 7.6 Hz, 1H), 7.05 (d, J = 7.6 Hz, 1H), 6.93 (d, J = 8.0 Hz, 1H), 6.84 (d, J = 8.4 Hz, 1H), 6.68 (t, J = 7.6 Hz, 1H), 5.19 (s, 2H). ^{13}C NMR (100 MHz, *DMSO-d_6*) (ppm): 161.6, 160.7, 160.6, 141.4, 139.6, 135.6, 133.7, 132.0, 130.8, 127.4, 127.4, 123.6, 122.2, 119.2, 117.1, 117.0, 112.0, 109.6.

*5.1.8. Benzo[k,l]xanthene-3,4-dicarboxylic anhydride (**12**) [35]*

11 (0.5 g, 0.0017 mol) was dissolved in glacial acetic acid (12 mL) and then hydrochloric acid (1 mL) and sodium nitrite solution (1.14 g, 0.016 mol in 4 mL water) were added at 0 °C. After 1 h copper sulfate solution (1.12 g, 0.007 mol in 20 mL water) was added. The reaction mixture was refluxed further for 0.5 h and cooled. The precipitate was filtered, washed with water and crystallized from DMF. Yellow solid, yield: 93.2%. M.p. 156–159 °C (m.p. 155–160 °C in literature).

*5.1.9. General procedure for the preparation of **13a–13d***

12 (0.29 g, 0.001 mol) was dissolved in 20 mL ethanol. After adding corresponding primary amine (0.003 mol), the mixture was stirred and refluxed for 2–3 h, then the solution was evaporated in vacuum and the residue was purified on silica gel chromatography.

*5.1.9.1. N-(N′,N′-dimethylamine-ethyl)-benzo[k,l]xanthene-3,4-naphthalimide (**13a**).* Yellow solid, yield: 85%, m.p. 191–192 °C. ^{1}H NMR (400 MHz, *$CDCl_3$*) (ppm): 8.60 (d, J = 8.0 Hz, 1H), 8.56 (d, J = 8.0 Hz, 1H), 8.04 (d, J = 8.0 Hz, 1H), 7.89 (d, J = 7.6 Hz, 1H), 7.54 (t, J = 7.6 Hz, 1H), 7.36 (d, J = 8.0 Hz, 2H), 7.26 (d, J = 8.4 Hz, 1H), 4.37 (t, J = 7.2 Hz, 2H), 2.74 (t, J = 7.2 Hz, 2H), 2.44 (s, 6H). ^{13}C NMR (100 MHz, *$CDCl_3$*) (ppm): 164.0, 163.7, 155.8, 151.9, 133.8, 133.4, 133.2, 132.1, 130.0, 125.0, 123.7, 119.9, 118.8, 118.1, 114.9, 114.8, 109.9, 56.9, 45.6, 37.9, 29.7. IR (KBr): 2937, 2770, 1645, 1594, 1380 cm^{-1}. HR-MS: $C_{22}H_{18}N_2O_3$ calculated: 358.1317, found: 358.1321.

*5.1.9.2. N-(N′,N′-dimethylamine-propyl)-benzo[k,l]xanthene-3,4-naphthalimide (**13b**).* Yellow solid, yield: 78%, m.p. 194–195 °C. ^{1}H NMR (400 MHz, *DMSO-d_6*) (ppm): 8.31 (d, J = 8.0 Hz, 2H), 8.18 (d, J = 8.4 Hz, 1H), 8.03 (d, J = 7.6 Hz, 1H), 7.59 (t, J = 7.6 Hz, 1H), 7.36 (d, J = 8.4 Hz, 2H), 7.25 (d, J = 8.4 Hz, 1H), 4.05 (t, J = 6.4 Hz, 2H), 3.12 (t, J = 4.0 Hz, 2H), 2.73 (s, 6H), 2.05 (t, J = 7.6 Hz, 2H). ^{13}C NMR (100 MHz, *DMSO-d_6*) (ppm): 163.5, 163.2, 155.3, 151.5, 133.7, 133.1, 133.0, 129.4, 125.8, 124.8, 119.5, 118.7, 118.2, 118.1, 116.1, 114.6, 110.3, 54.9, 42.5, 37.4, 23.4. IR (KBr): 2929, 2766, 1588, 1657, 1382, 769 cm^{-1}; HR-MS: $C_{23}H_{20}N_2O_3$ calculated: 372.1474, found 372.1473.

*5.1.9.3. N-(n-butyl)-benzo[k,l]xanthene-3,4-naphthalimide (**13c**).* Yellow solid, yield: 75%, m.p. 181–182 °C. ^{1}H NMR (400 MHz, *$CDCl_3$*) (ppm): 8.62 (d, J = 7.6 Hz, 1H), 8.58 (d, J = 8.4 Hz, 1H), 8.06 (d, J = 7.6 Hz, 1H), 7.91 (d, J = 7.2 Hz, 1H), 7.54 (t, J = 7.6 Hz, 1H), 7.35 (t, J = 8.0 Hz, 2H), 7.27 (d, J = 10.0 Hz, 1H), 4.21 (t, J = 7.2 Hz, 2H), 1.79–1.71 (m, 2H), 1.53–1.44 (m, 2H), 1.01 (t, J = 6.8 Hz, 3H). ^{13}C NMR (100 MHz, *$CDCl_3$*) (ppm): 155.7, 151.9, 133.7, 133.3, 133.1, 132.0, 129.9, 125.0, 123.7, 119.1, 118.8, 118.1, 114.8, 109.8, 40.2, 30.2, 20.5, 13.9. IR (KBr): 2947, 2867, 1855, 1386, 759 cm^{-1}; HR-MS: $C_{22}H_{17}NO_3$ calculated: 343.1208, found: 343.1206.

*5.1.9.4. N-(2′-piperazidine-ethyl)-benzo[k,l]xanthene-3,4-naphthalimide (**13d**).* Yellow solid, yield: 82%, m.p. 198–200 °C. ^{1}H NMR (400 MHz, *$CDCl_3$–CD_3OD*) (ppm): 8.58 (d, J = 8.0 Hz, 1H), 8.53 (d, J = 8.4 Hz, 1H), 8.08 (d, J = 7.6 Hz, 1H), 7.96 (d, J = 7.6 Hz, 1H), 7.54 (t, J = 7.2 Hz, 1H), 7.37 (brs, 2H), 7.28 (t, J = 7.6 Hz, 1H), 4.31 (t, J = 6.8 Hz, 2H), 3.93–3.87 (m, 2H), 3.01 (brs, 4H), 2.74 (brs, 4H). ^{13}C NMR (100 MHz, *$CDCl_3$–CD_3OD*) (ppm): 164.2, 163.9, 156.1, 151.9, 134.0, 133.9, 133.4, 132.3, 130.0, 125.2, 123.8, 118.9, 118.7, 118.1, 115.0, 110.0, 55.6, 51.5, 44.3, 37.0. IR (KBr): 2921, 2855, 1688, 1660, 1590, 765 cm^{-1}. HR-MS: $C_{24}H_{21}N_3O_3$ calculated: 399.1583, found: 399.1576.

*5.1.10. 4-Phenoxy-3-nitro-dicarboxylic anhydride (**14**) [23]*

A mixture of **4** (9.8 g, 0.030 mol), phenol (1.8 mL, 0.0175 mol) and sodium hydride (1.3 g, 0.054 mol) was refluxed in pyridine (220 mL) for 5 h. The solution was concentrated, filtered, and washed with water. Pale yellow solid, yield: 97%, m.p. 289.0–289.9 °C (m.p. 287 °C in literature). ^{1}H NMR (400 MHz, *DMSO-d_6*) (ppm): 8.99 (s, 1H), 8.73 (d, J = 7.2 Hz, 1H), 8.52 (d, J = 8.4 Hz, 1H), 8.04 (t, J = 8.0 Hz, 1H), 7.40 (t, J = 7.6 Hz, 2H), 7.17 (t, J = 7.2 Hz, 1H), 6.99 (d, J = 8.0 Hz, 2H). ^{13}C NMR (100 MHz, *DMSO-d_6*) (ppm): 160.3, 159.5, 158.4, 149.6, 140.7, 135.7, 133.1, 131.4, 130.8, 130.3, 128.0, 126.9, 124.3, 120.9, 118.1, 116.0.

*5.1.11. 4-Phenoxy-3-amino-dicarboxylic anhydride (**15**) [23]*

14 (5.24 g, 0.016 mol) was added to $SnCl_2 \cdot 2H_2O$ (29 g, 0.129 mol) in hydrochloric acid (36%, 100 mL). The reaction mixture was stirred at 85 °C for 2 h. Then the reaction was cooled and filtered. The residue was washed with water and recrystallized from pyridine. Yellow solid, yield: 79.7%, m.p. 261.2–262.3 °C (m.p. 258–259 °C in literature). ^{1}H NMR (400 MHz, *DMSO-d_6*) (ppm): 8.25 (s, 1H), 8.17 (d, J = 6.8 Hz, 1H), 7.94 (d, J = 8.0 Hz, 1H), 7.68 (t, J = 7.6 Hz, 1H), 7.33 (t, J = 7.2 Hz, 2H), 7.07 (t, J = 6.0 Hz, 1H), 6.87 (d, J = 7.6 Hz, 2H), 6.02 (s, 2H). ^{13}C NMR (100 MHz, *DMSO-d_6*) (ppm): 161.4, 160.8, 157.6, 141.0, 136.5, 130.4, 128.3, 128.0, 127.5, 127.1, 125.1, 124.3, 123.0, 119.7, 117.0, 115.6.

*5.1.12. Benzo[b]furano[2,1-c] dicarboxylic anhydride (**16**) [23]*

The solution of $NaNO_2$ (0.545 g, 0.008 mol) in concentrated sulfuric acid (32.7 mL) was added dropwise with glacial acetic acid (4.87 mL) at −5 to 0 °C and then added with **15** (2 g, 0.007 mol) in batches. After 2 h, the solution was added dropwise to the mixed solution (74 g copper sulfate, 100 mL glacial acetic acid, 800 mL water) and then continued to reflux for 0.5 h. The resulting suspension was cooled, filtered and washed with water. The solid was purified on silica gel chromatography (petroleum ether/ethyl acetate, 5:1). Yellow solid, yield: 61%, m.p. 147–149 °C (m.p. 145–146 °C in literature). ^{1}H NMR (400 MHz, *DMSO-d_6*) (ppm): 9.43 (s, 1H), 8.93 (d, J = 8.4 Hz, 1H), 8.63 (d, J = 7.2 Hz, 1H), 8.52 (d, J = 7.6 Hz, 1H), 8.09 (t, J = 8.0 Hz, 1H), 7.99 (d, J = 8.4 Hz, 1H), 7.70 (t, J = 8.0 Hz, 1H), 7.59 (t, J = 7.6 Hz, 1H).

*5.1.13. General procedure for the preparation of **17a–17d***

16 (0.29 g, 0.001 mol) was dissolved in 20 mL ethanol. After adding corresponding primary amine (0.003 mol), the mixture was stirred and refluxed for 2 h. Then the solution was evaporated in vacuum and the residue was purified on silica gel chromatography.

*5.1.13.1. N-(N′,N′-dimethylamine-ethyl)-benzo[b]furano[2,1-c]naphthalimide (**17a**).* Yellow solid, yield: 91%, m.p. 156–157 °C. ^{1}H NMR (400 MHz, *$CDCl_3$*) (ppm): 9.15 (s, 1H), 8.74 (d, J = 8.4 Hz, 1H), 8.67 (d,

J = 7.2 Hz, 1H), 8.10 (d, J = 7.6 Hz, 1H), 7.89 (t, J = 8.0 Hz, 1H), 7.77 (d, J = 8.0 Hz, 1H), 7.60 (t, J = 8.0 Hz, 1H), 7.51 (t, J = 7.6 Hz, 1H), 4.42 (t, J = 7.2 Hz, 2H), 2.80 (t, J = 6.4 Hz, 2H), 2.47 (s, 6H). ^{13}C NMR (100 MHz, *CDCl*$_3$) (ppm): 164.3, 164.2, 156.5, 155.2, 130.9, 127.9, 127.8, 127.2, 127.1, 125.5, 124.2, 124.0, 123.2, 121.0, 120.7, 119.2, 118.0, 112.2, 56.9, 45.6, 38.0. IR (KBr): 2925, 2848, 2361, 1696, 1337 cm^{-1}. HR-MS: $C_{22}H_{18}N_2O_3$ calculated: 358.1317, found: 358.1317.

*5.1.13.2. N-(N′,N′-dimethylamine-propyl)-benzo[b]furano[2,1-c] naphthalimide (**17b**).* Yellow solid, yield: 85%, m.p. 185–186 °C. ^{1}H NMR (400 MHz, *CDCl*$_3$–*CD*$_3$*OD*) (ppm): 9.12 (s, 1H), 8.77 (d, J = 8.0 Hz, 1H), 8.63 (d, J = 7.6 Hz, 1H), 8.12 (d, J = 7.6 Hz, 1H), 7.92 (t, J = 8.4 Hz, 1H), 7.77 (t, J = 8.4 Hz, 1H), 7.61 (t, J = 8.0 Hz, 1H), 7.52 (t, J = 6.8 Hz, 1H), 4.31 (t, J = 6.4 Hz, 2H), 3.09 (t, J = 7.6 Hz, 2H), 3.77 (s, 6H), 2.24–2.18 (m, 2H). ^{13}C NMR (100 MHz, *CDCl*$_3$–*CD*$_3$*OD*) (ppm): 164.6, 164.4, 156.5, 155.4, 131.1, 128.1, 127.7, 127.6, 127.3, 125.7, 124.3, 123.6, 122.6, 120.9, 120.9, 119.2, 117.4, 112.2, 56.0, 43.3, 37.5, 29.6, 24.1. IR (KBr): 2921, 2844, 2754, 1657, 1345 cm^{-1}. HR-MS: $C_{23}H_{20}N_2O_3$ calculated: 372.1474, found: 372.1465.

*5.1.13.3. N-(n-butyl)-benzo[b]furano[2,1-c]naphthalimide (**17c**).* Yellow solid, yield: 81%, m.p. 151–152 °C. ^{1}H NMR (400 MHz, *CDCl*$_3$) (ppm): 9.21 (s, 1H), 8.78 (d, J = 8.0 Hz, 1H), 8.71 (d, J = 7.2 Hz, 1H), 8.15 (d, J = 7.6 Hz, 1H), 7.92 (t, J = 8.0 Hz, 1H), 7.80 (d, J = 8.4 Hz, 1H), 7.62 (t, J = 8.0 Hz, 1H), 7.53 (t, J = 7.6 Hz, 1H), 4.26 (t, J = 7.6 Hz, 2H), 1.83–1.75 (m, 2H), 1.56–1.47 (m, 2H), 1.03 (t, J = 7.6 Hz, 3H). ^{13}C NMR (100 MHz, *CDCl*$_3$) (ppm): 164.3, 164.2, 156.5, 155.2, 130.9, 127.8, 127.2, 127.1, 125.4, 124.2, 124.0, 123.3, 121.0, 120.8, 119.3, 118.2, 112.2, 40.4, 30.3, 20.4, 13.9. IR (KBr): 2921, 2830, 1700, 1650, 1330 cm^{-1}. HR-MS: $C_{22}H_{17}NO_3$ calculated: 343.1208, found: 343.1303.

*5.1.13.4. N-(2′-piperazidine-ethyl)-benzo[b]furano[2,1-c]naphthalimide (**17d**).* Yellow solid, yield: 76%, m.p. 195–196 °C. ^{1}H NMR (400 MHz, *CDCl*$_3$–*CD*$_3$*OD*) (ppm): 9.14 (s, 1H), 8.77 (d, J = 8.4 Hz, 1H), 8.64 (d, J = 7.2 Hz, 1H), 8.11 (d, J = 8.0 Hz, 1H), 7.90 (t, J = 8.0 Hz, 1H), 7.76 (d, J = 8.4 Hz, 1H), 7.58 (t, J = 8.0 Hz, 1H), 7.49 (t, J = 7.2 Hz, 1H), 4.36 (t, J = 6.4 Hz, 2H), 2.97 (brs, 4H), 2.77 (t, J = 6.8 Hz, 2H), 2.72 (brs, 4H). ^{13}C NMR (100 MHz, *CDCl*$_3$–*CD*$_3$*OD*) (ppm): 164.6, 164.4, 156.5, 155.3, 131.0, 128.0, 127.7, 127.4, 127.3, 125.6, 124.3, 123.8, 122.9, 120.9, 120.9, 119.3, 117.7, 112.2, 55.8, 52.2, 44.5, 37.2. IR (KBr): 2925, 2855, 2357, 1660, 1365 cm^{-1}. HR-MS: $C_{24}H_{21}N_3O_3$ calculated: 399.1583, found: 399.1588.

5.2. kDNA decatenation assay

Topoisomerase II activity was measured by the ATP-dependent decatenation of kDNA according to the manufacturer's instructions (TopoGEN, Florida, USA). 0.1 μg kDNA, 1 unit of human topo IIa (TopoGEN) and the indicated concentrations of compounds were incubated for 30 min at 37 °C in 50 mM Tris–HCl (pH 8), 150 mM NaCl, 10 mM $MgCl_2$, 2 mM ATP, 0.5 mM DTT in a total volume of 20 μL. The reactions were stopped by the addition of 2 μL 10% SDS and 2 μL 6 × loading dye solution (Fermentas). Samples were then electrophoresed in 0.8% agarose gel in TAE buffer for 50 min at 120 V. The gel was stained with ethidium bromide at room temperature and photographed with UV transilluminator.

5.3. DNA relaxation assay

Topoisomerase I activity was assayed by relaxation of supercoiled pBR322 DNA according to the manufacturer's instructions (Takara, Dalian, China). Topo I (calf thymus), buffer, BSA, loading buffer and supercoiled pBR322 DNA were all from TaKaRa Biotechnology CO., Ltd. 0.5 μg supercoiled pBR322 DNA, 0.1 units of topoisomerase I and the indicated concentrations of compounds were incubated for 30 min at 37 °C in DNA topoisomerase I buffer with 0.01% bovine serum albumin, in a total volume of 20 μL. The reactions were stopped by the addition of 2 μL 10% SDS and 2 μL 6 × loading dye solution (Fermentas). Samples were then electrophoresed in 0.8% agarose gel in TAE buffer for 35 min at 120 V. The gel was stained with ethidium bromide at room temperature and photographed with UV transilluminator.

5.4. DNA intercalating assay by CD spectra

ctDNA was purchased from Sigma Aldrich and used without further purification. The concentrations of compounds and calf thymus DNA were 20 μM and 100 μM respectively in 20 mM Tris–HCl buffer, pH 7.5 and DMSO (1% by volume). The CD measurements were performed on a Chirascan™ CD Spectrometer (Applied Photophysics Ltd, England) using 1 cm quartz cell in the wavelength range of 240–300 nm.

5.5. DNA intercalating assay by fluorescence quenching

The fluorescence spectra were obtained using a Varian Cary Eclipse fluorescence spectrophotometer at 25 °C. The concentrations of compounds and calf thymus DNA were 20 μM and 0–150 μM respectively in 20 mM Tris–HCl buffer, pH 7.5 and DMSO (1% by volume), the solution in a final volume of 10 mL, which was used for fluorescence-quenching experiments. And an equilibrium period of 1 h for constant stirring at 25 °C in the dark of the mixed solution was allowed before recording each spectrum. The association constants (Ka's) were derived according to the equation $I = I_0 + \{(I_\infty - I_0)/2[Q]_0\} \times \{([DNA]_0 + [Q]_0 + 1/Ka) - \{([DNA]_0 + [Q]_0 + 1/Ka)^2 - 4[DNA]_0[Q]_0\}^{1/2}\}$, wherein I_0, I and I_∞ represent the fluorescence intensities of compounds alone, the sample and DNA totally bound, respectively. $[DNA]_0$ and $[Q]_0$ were the initial analytical concentrations of DNA and the agents, respectively.

Acknowledgments

This work is financially supported by the National Basic Research Program of China (973 Program, 2010CB126100), the National High Technology Research and Development Program of China (863 Program, 2011AA10A207), the China 111 Project (grant B07023), the Fundamental Research Funds for the Central Universities, and the Shanghai Committee of Science and Technology [grant 11DZ2260600]. We thank Chenghui Xu for antiproliferation assay against A549 and P388 cancer cell lines.

Appendix A. Supplementary data

Supplementary data related to this article can be found at http://dx.doi.org/10.1016/j.ejmech.2012.12.039.

References

[1] J. Feigon, W.A. Denny, W. Leupin, D.R. Kearns, Interaction of antitumor drugs with natural DNA: ^{1}H NMR study of binding mode and kinetics, J. Med. Chem. 27 (1984) 450–465.
[2] L.H. Hurley, DNA and its associated processes as targets for cancer therapy, Nat. Rev. Cancer 2 (2002) 188–200.
[3] C.H. Tseng, C.C. Tzeng, C.L. Yang, P.J. Lu, H.L. Chen, H.Y. Li, Y.C. Chuang, C.N. Yang, Y.L. Chen, Synthesis and antiproliferative evaluation of certain indeno[1,2-*c*]quinoline derivatives. Part 2, J. Med. Chem. 53 (2010) 6164–6179.
[4] M.F. Braña, Butyramiden und verfahren zu dessen herstelling, Patent DE2318136, 1973.
[5] E. Van Quaquebeke, T. Mahieu, P. Dumont, J. Dewelle, F. Ribaucour, G. Simon, S. Sauvage, J.F. Gaussin, J. Tuti, M. El Yazidi, F. Van Vynckt, T. Mijatovic,

F. Lefranc, F. Darro, R. Kiss, 2,2,2-Trichloro-*N*-({2-[2-(dimethylamino)ethyl]-1,3-dioxo-2,3-dihydro-1*H*-benzo[de]isoquinolin5-yl} carbamoyl) acetamide (UNBS3157), a novel nonhematotoxic naphthalimide derivative with potent antitumor activity, J. Med. Chem. 50 (2007) 4122–4134.
[6] M. Lv, H. Xu, Overview of naphthalimide analogs as anticancer agents, Curr. Med. Chem. 16 (2009) 4797–4813.
[7] S. Li, W. Zhong, Z. Li, X. Meng, Unprecedented synthesis, in vitro and in vivo anti-cancer evaluation of novel triazolonaphthalimide derivatives, Eur. J. Med. Chem. 47 (2012) 546–552.
[8] L. Ingrassia, F. Lefranc, R. Kiss, T. Mijatovic, Naphthalimides and azonafides as promising anti-cancer agents, Curr. Med. Chem. 16 (2009) 1192–1213.
[9] V.K. Malviya, P.Y. Liu, D.S. Alberts, E.A. Surwit, J.B. Craig, E.V. Hanningan, Evaluation of amonafide in cervical cancer, phase II study, Am. J. Clin. Oncol. 15 (1992) 41–44.
[10] S.M. Sami, R.T. Dorr, D.S. Alberts, W.A. Remers, 2-substituted 1,2-dihydro-3*H*-dibenz[de,h]isoquinoline-1,3-diones. A new class of antitumor agent, J. Med. Chem. 36 (1993) 765–770.
[11] S.M. Sami, R.T. Dorr, A.M. Solyom, D.S. Alberts, W.A. Remers, Amino-substituted 2-[2′-(dimethylamino)ethyl]-1,2-dihydro-3*H*-dibenz[de,h] isoquinoline-1,3-diones. Synthesis, antitumor activity, and quantitative structure–activity relationship, J. Med. Chem. 38 (1995) 983–993.
[12] M.F. Braña, M. Cacho, M.A. Garcia, B. de Pascual-Teresa, A. Ramos, N. Acero, F. Llinares, D. Munoz-Mingarro, C. Abradelo, M.F. Rey-Stolle, M. Yuste, Synthesis, antitumor activity, molecular modeling, and DNA binding properties of a new series of imidazonaphthalimides, J. Med. Chem. 45 (2002) 5813–5816.
[13] M.F. Braña, M. Cacho, M.A. Garcia, B. de Pascual-Teresa, A. Ramos, M.T. Dominguez, J.M. Pozuelo, C. Abradelo, M.F. Rey-Stolle, M. Yuste, M. Banez-Coronel, J.C. Lacal, New analogues of amonafide and elinafide, containing aromatic heterocycles: synthesis, antitumor activity, molecular modeling, and DNA binding properties, J. Med. Chem. 47 (2004) 1391–1399.
[14] M.F. Braña, M. Cacho, A. Ramos, M.T. Dominguez, J.M. Pozuelo, C. Abradelo, M.F. Rey-Stolle, M. Yuste, C. Carrasco, C. Bailly, Synthesis, biological evaluation and DNA binding properties of novel mono and bisnaphthalimides, Bioorg. Med. Chem. 1 (2003) 648–654.
[15] Y.G. Li, Y.F. Xu, X.H. Qian, B. Qu, Naphthalimide-thiazoles as novel photonucleases: molecular design, synthesis, and evaluation, Tetrahedron Lett. 45 (2004) 1247–1251.
[16] X.H. Qian, Z.G. Li, Q. Yang, Highly efficient antitumor agents of heterocycles containing sulfur atom: linear and angular thiazonaphthalimides against human lung cancer cell in vitro, Bioorg. Med. Chem. 15 (2007) 6846–6851.
[17] X. Liang, A.B. Wu, Y.F. Xu, K. Xu, J.W. Liu, X.H. Qian, B1, a novel naphthalimide-based DNA intercalator, induces cell cycle arrest and apoptosis in HeLa cells via p53 activation, Investig. New Drug 29 (2011) 646–658.
[18] L.J. Xie, Y.F. Xu, F. Wang, J.W. Liu, X.H. Qian, J.N. Cui, Synthesis of new amonafide analogues via coupling reaction and their cytotoxic evaluation and DNA-binding studies, Bioorg. Med. Chem. 17 (2009) 804–810.
[19] X. Qian, Y. Li, Y. Xu, Y. Liu, B. Qu, Highly-efficient DNA photocleavers with long wavelength absorptions: thio-heterocyclic fused naphthalimides containing aminoalkyl side chains, Bioorg. Med. Chem. Lett. 14 (2004) 2665–2668.
[20] Y. Xu, B. Qu, X. Qian, Y. Li, Five-member thio-heterocyclic fused naphthalimides with aminoalkyl side chains: intercalation and photocleavage to DNA, Bioorg. Med. Chem. Lett. 15 (2005) 1139–1142.
[21] W. Yao, X. Qian, Oxazolonaphthalimides and their hydroperoxides: photophysical and photobiological properties, Dyes Pigm. 48 (2001) 43–47.
[22] H. Yin, W. Zhu, Y. Xu, M. Dai, X. Qian, Y. Li, J. Liu, Novel aliphatic N-oxide of naphthalimides as fluorescent markers for hypoxic cells in solid tumor, Eur. J. Med. Chem. 46 (2011) 3030–3037.
[23] X. Qian, J. Cui, R. Zhang, Intramolecular aromatic 1,5-hydrogen transfer in preparation of oxacyclic naphthalic anhydride via unusual Pschorr cyclisation, Chem. Commun. (2001) 2656–2657.
[24] Z. Chen, X. Liang, H.Y. Zhang, H. Xie, J.W. Liu, Y.F. Xu, W.P. Zhu, Y. Wang, X. Wang, S.Y. Tan, D. Kuang, X.H. Qian, A new class of naphthalimide-based antitumor agents that inhibit topoisomerase II and induce lysosomal membrane permeabilization and apoptosis, J. Med. Chem. 53 (2010) 2589–2600.
[25] I. Ott, Y.F. Xu, J.W. Liu, M. Kokoschka, M. Harlos, W.S. Sheldrick, X.H. Qian, Sulfur-substituted naphthalimides as photoactivatable anticancer agents: DNA interaction, fluorescence imaging, and phototoxic effects in cultured tumor cells, Bioorg. Med. Chem. 16 (2008) 7107–7116.
[26] X.L. Li, Y.J. Lin, Y.K. Yuan, K. Liu, X.H. Qian, Novel efficient anticancer agents and DNA-intercalators of 1,2,3-triazol-1,8-naphthalimides: design, synthesis, and biological activity, Tetrahedron 67 (2011) 2299–2304.
[27] H. Zhu, M. Huang, F. Yang, Y. Chen, Z.H. Miao, X.H. Qian, Y.F. Xu, Y.X. Qin, H.B. Luo, X. Shen, M.Y. Geng, Y.J. Cai, J. Ding, R16, a novel amonafide analogue, induces apoptosis and G(2)-M arrest via poisoning topoisomerase II, Mol. Cancer Ther. 6 (2007) 484–495.
[28] M.G. Ferlin, C. Marzano, V. Gandin, S. Dall'Acqua, L. Dalla Via, DNA binding ellipticine analogues: synthesis, biological evaluation, and structure–activity relationships, ChemMedChem 4 (2009) 363–377.
[29] W. Liu, L. Zhu, W. Guo, C. Zhuang, Y. Zhang, C. Sheng, P. Cheng, J. Yao, W. Wang, G. Dong, S. Wang, Z. Miao, W. Zhang, Synthesis and biological evaluation of novel 7-acyl homocamptothecins as topoisomerase I inhibitors, Eur. J. Med. Chem. 46 (2011) 2408–2414.
[30] M. López-Lázaro, E. Willmore, A. Jobson, K.L. Gilroy, H. Curtis, K. Padget, C.A. Austin, Curcumin induces high levels of topoisomerase I- and II-DNA complexes in K562 leukemia cells, J. Nat. Prod. 70 (2007) 1884–1888.
[31] C. Bailly, C. Carrasco, A. Joubert, C. Bal, N. Wattez, M.P. Hildebrand, A. Lansiaux, P. Colson, C. Houssier, M. Cacho, A. Ramos, M.F. Braña, Chromophore-modified bisnaphthalimides: DNA recognition, topoisomerase inhibition, and cytotoxic properties of two mono- and bis-furonaphthalimides, Biochemistry 42 (2003) 4136–4150.
[32] J. Wang, A.B. Wu, Y.F. Xu, J.W. Liu, X.H. Qian, M(2)-A induces apoptosis and G(2)-M arrest via inhibiting PI3 K/Akt pathway in HL60 cells, Cancer Lett. 283 (2009) 193–202.
[33] X. Liang, K. Xu, Y.F. Xu, J.W. Liu, X.H. Qian, B1-induced caspase-independent apoptosis in MCF-7 cells is mediated by down-regulation of Bcl-2 via p53 binding to P2 promoter TATA box, Toxicol. Appl. Pharmacol. 256 (2011) 52–61.
[34] Q. Yang, P. Yang, X.H. Qian, L.P. Tong, Naphthalimide intercalators with chiral amino side chains: effects of chirality on DNA binding, photodamage and antitumor cytotoxicity, Bioorg. Med. Chem. 13 (2008) 6210–6213.
[35] Y.Sh. Bcheshtiha, M.M. Heravi, F.A. Salehi, Synthesis of benzimid-azoxanthenoisoquinolinones, new intermediates and dyes for synthetic-polymer fibres, Indian J. Chem. 37B (1998) 1177–1179.